RAPID COMMUNICATIONS

PHYSICAL REVIEW B VOLUME 35, NUMBER 5 15 FEBRUARY 1987-I

Picosecond Raman scattering from photoexcited plasmas in InP with spatial and temporal resolution

Jeff F. Young and Kam Wan
Division of Physics, National Research Council of Canada, Ottawa, Ontario, Canada K1A 0R6
(Received 24 October 1986)

Picosecond, time-resolved Raman scattering spectra from photoexcited plasmon-phonon modes in semi-insulating InP are presented. Spectra of plasmas ranging in density from 0.1×10^{17} to 5.0×10^{17} cm^{-3} are quantitatively fitted by extending equilibrium n-type plasmon-phonon scattering theories to include contributions from free holes. A novel application of time-resolved Raman scattering to measure the ambipolar diffusion coefficient and surface recombination velocity of nonequilibrium semiconductor plasmas is demonstrated.

From the viewpoint of semiconductor physics, time-resolved Raman scattering (TRRS) is a demonstrated, powerful tool for directly measuring LO-phonon lifetimes[1] and indirectly determining electronic intervalley scattering[2] as well as energy relaxation rates.[3] The theory of Luzzi and co-workers[4] suggests that Raman scattering from the electronic system itself should, in principle, provide even more direct information concerning the evolution of nonequilibrium electron-hole plasmas (NEEHP's) in semiconductors. From a Raman scattering point of view, optically pumped semiconductors are of special interest since they should provide an ideal testing ground for existing theories[4-6] of light scattering from both classical and quantum-mechanical multicomponent plasmas. However, in order for TRRS to develop into a useful probe of semiconductor plasma properties, the abilitiy to quantitatively fit actual light scattering data from NEEHP's is requisite.

There have been several reported Raman scattering studies of optically excited electron-hole plasmas in GaAs,[3,7-11] GaP,[12] and InP.[13] Most of the work has concentrated on the high-energy portion of the spectrum associated with coupled plasmon–LO-phonon modes. In general, the measured energies of the coupled modes depends on the plasma density and can, in principle, be used to directly measure this quantity. In practice, with the exception of the work of Nather and Quagliano,[10] the ability to *quantitatively* fit coupled-mode spectra from electron-hole plasmas denser than $\sim1\times10^{17}$ cm^{-3} has not been demonstrated. This situation can be attributed, at least in part, to complications introduced by scattering from temporally varying and/or spatially inhomogeneous plasmas.

By using special lithographed disks on a multilayer GaAs-$Al_xGa_{1-x}As$ sample to minimize spatial averaging, Nather and Quagliano[10] have obtained quantitative fits to data from steady-state plasmas as dense as 5×10^{17} cm^{-3}.

In this paper, we present the results of picosecond Raman scattering experiments from optically excited electron-hole plasmas in InP with densities ranging from 0.1×10^{17} to 5.0×10^{17} cm^{-3}. The use of separate picosecond laser sources to produce and probe the NEEHP's reduces both spatial- and temporal-averaging effects to negligible levels without the need of lithography. The key points of a model developed to fit the coupled plasmon–LO-phonon portion of the spectra, and hence extract the carrier density and scattering rates, are discussed. Finally, a novel application of picosecond TRRS to measure the ambipolar diffusion coefficient and surface recombination velocity of NEEHP's in InP is demonstrated.

The light scattering experiments were performed on a chemically polished (2% bromine methanol) semi-insulating InP (100) surface. The beam used to generate the NEEHP's was obtained by frequency doubling the output of a Quantronix 416 cw mode-locked YAG (yttrium aluminum garnet) laser. The photon energy was 2.33 eV, the repetition rate 76 MHz, the pulse duration 82 psec [full width at half maximum (FWHM)] and the average power was kept at 480 mW. The probe beam was generated by using part of the 2.33-eV YAG beam to synchronously pump a Coherent 700 dye laser operated with Rh590 dye. The pulse duration of the dye laser was 4 psec (FWHM) at 565.4 nm, the average power was 20 mW, and there was less than 2-psec jitter between the dye and YAG laser pulses.[14] Both beams were p polarized with incident polarization parallel to the (010) plane. The pump beam was focused on the sample to an elliptical spot size of 200×220 μm^2 and the probe beam was focused concentric with the pump beam to a spot size of 60×90 μm^2. The spot sizes were accurately measured with an imaging system in order to quantitatively calculate the expected carrier density generated by the pump pulse. The scattered light from the dye laser was collected normal to the surface and analyzed before entering a Spex Triplemate spectrometer with a cooled, unintensified charge coupled array detector. The Raman scattering geometry was thus close to $z(x,y)\bar{z}$. All of the spectra reported here were obtained at room temperature, using a two-hour exposure.

The Stokes component of the light scattered from the dye laser pulses was recorded as a function of the delay time between the arrival of the pump and probe pulses at the sample surface. Although the dye laser was not strongly resonant with any band gaps of InP, the Raman signal was superimposed on a slowly varying luminescent background. For all delay times, the Raman spectrum was featureless except in the vicinity of the unscreened LO-phonon mode at 345.5 cm^{-1}. The spectrum of the unscreened LO-phonon mode as obtained with no pump pulse present is shown in Fig. 1(a). The spectrum obtained with the pump beam present and the probe beam

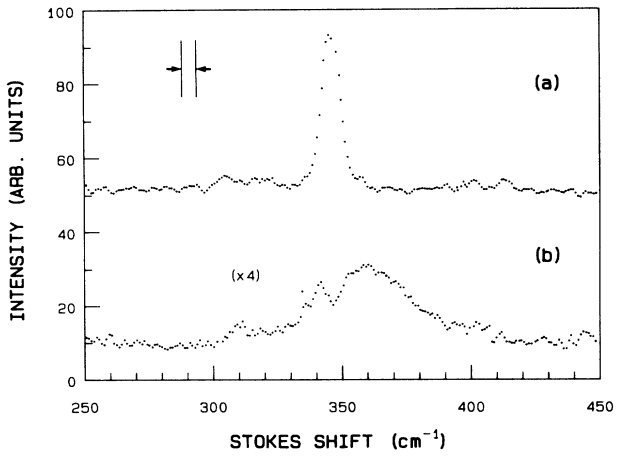

FIG. 1. (a) The unscreened LO-phonon spectrum obtained with no pump beam, and (b) the coupled-mode spectrum obtained with the probe beam delayed 62 psec with respect to the pump beam.

delayed to strike the surface 62 psec after the arrival of the peak of the pump pulse is shown in Fig. 1(b). The changes in energy, linewidth, and intensity of the peak in the spectrum obtained from the photoexcited surface are all qualitatively similar to the results obtained from equilibrium n-type plasmon-phonon modes.[6] Table I summarizes the measured intensity, shift, and width of the coupled mode peaks, similar to Fig. 1(b), as a function of the delay time between pulses.

In order to fit the peak positions and widths of the spectra, we adopted existing formalisms[15,16] developed to treat the scattering from coupled plasmon-phonon modes in equilibrium n-type samples, and modified them to include the contribution of free holes. For the scattering geometry used in the present experiments, only the deformation potential and electro-optic terms in the nonlinear susceptibility could contribute significantly to the nonlinear polarization responsible for the observed signals near 345 cm^{-1}. Thus we took the differential scattering cross section to be

$$\frac{d^2\sigma}{d\Omega d\omega} \propto (d_u^2\langle u^2\rangle + 2d_u d_E\langle uE\rangle + d_E^2\langle E^2\rangle) \ , \qquad (1)$$

where d_u and d_E are the deformation potential and electro-optic nonlinear susceptibility coefficients of InP, u and E represent the phonon coordinate and macroscopic electric field associated with the coupled modes, and the angular brackets represent thermodynamic averages of the quantities contained within. Following the derivation in Ref. 15, the averages of the fluctuating quantities in Eq. (1) can be expressed in terms of the linear response functions, or susceptibilities, of the ionic and electronic components of the excited semiconductor. Thus we have

$$\begin{aligned}
\langle u^2\rangle &= [\hbar(n+1)/2\pi]\,\mathrm{Im}[(4\pi)^2\chi_I(\varepsilon_\infty+4\pi\chi_e)/\varepsilon_\infty^2\varepsilon] \ , \\
\langle E^2\rangle &= [\hbar(n+1)/2\pi]\,\mathrm{Im}[-4\pi/\varepsilon] \ , \\
\langle uE\rangle &= [\hbar(n+1)/2\pi]\,\mathrm{Im}[(4\pi)^2\chi_I/\varepsilon_\infty\varepsilon] \ , \\
\varepsilon &= \varepsilon_\infty+4\pi(\chi_I+\chi_e) \ ,
\end{aligned} \qquad (2)$$

with

$$\chi_I = (4\pi)^{-1}(\varepsilon_0-\varepsilon_\infty)\omega_t^2(\omega_t^2-\omega^2-i\omega\Gamma_I)^{-1}$$

representing the ionic susceptibility and $\chi_e = \chi_c+\chi_{\mathrm{LH}}+\chi_{\mathrm{HH}}+\chi_{\mathrm{inter}}$ representing the susceptibility of the electrons and holes. ε_0 and ε_∞ are the static and high-frequency dielectric constants of the material, ω_t is the TO-phonon energy, Γ_I is a phenomenological damping constant associated with the phonon lifetime, and n is a thermal occupation factor. χ_c, χ_{LH}, and χ_{HH} are the intraband contributions from the conduction, light-hole, and heavy-hole bands, respectively. Within the random-phase approximation these intraband terms take the form[5]

$$\chi_i(K,\omega) = -\left\{\frac{N_i e^2}{m_i^*}\left[1+\left(\frac{3k_BT}{m_i^*\omega^2}\right)K^2\right]\right\}[\omega(\omega+i\Gamma_i)]^{-1} \ , \qquad (3)$$

where i refers to the band (c, LH, HH), N_i represents the density, m_i^* the effective mass, K the wave vector of the disturbance, and k_BT the thermal energy. The phenomenological damping term Γ_i turns out to be much larger than the Landau damping term which is omitted in Eq. (3). The intervalence band term χ_{inter} was calculated numerically using the expressions given in Refs. 17 and 18 (in the limit of $K\rightarrow 0$), with proper account taken for the room-temperature distribution functions. Details of this calculation will be published elsewhere.

The ratio of deformation potential to electro-optic susceptibility terms was estimated by measuring the ratio of integrated scattering intensities of the LO and TO phonon peaks [from (100) and (110) surfaces, respectively] and using the relation[19]

$$\frac{d\sigma_{\mathrm{LO}}}{d\sigma_{\mathrm{TO}}} = \frac{\omega_t}{\omega_l}\left(1+\frac{\omega_l^2-\omega_t^2}{C\omega_t^2}\right)^2 \ ,$$

where

$$C = \frac{(\varepsilon_\infty-\varepsilon_0)d_u}{\varepsilon_\infty d_E}$$

is the "Faust-Henry coefficient."

In order to have only one variable parameter associated with electronic damping, we assumed that the damping constants Γ_i were proportional to a power of their respec-

TABLE I. Summary of coupled-mode spectral characteristics.

Delay time (psec)	Intensity (arbitrary)	Shift (cm^{-1})	Width (cm^{-1})	Density (10^{17} cm^{-3})
−73.0	49.1	346.1	8	0.1
−39.1	15.7	356.9	29	3.0
−5.2	11.7	360.8	47	4.1
28.6	10.0	364.7	50	4.8
62.5	13.7	359.0	35	3.5
96.4	16.7	355.4	29	2.8
130.2	18.3	353.9	26	2.5
164.1	23.1	351.2	19	1.8

tive effective masses. The appropriate power $\frac{3}{2} \pm \frac{1}{2}$ was found by requiring that all of the spectra obtained for a given pump-beam fluence be fit with the same damping parameters. A summary of the fixed parameters used in the fitting procedure is listed in Table II. Thus only two parameters, the plasma density and the electron damping constant, could be varied to obtain fits of the observed spectra. The quality of the fit obtained for the spectrum taken at a delay time of 62 psec with respect to the peak of the pump pulse is shown in Fig. 2. A density of 3.5×10^{17} cm^{-3} and an electron damping constant of 280 cm^{-1} were used to obtain the solid curve in Fig. 2. Fits of similar quality were obtained for all delay times using the same damping constant and varying only the density. The actual spectra generally tend to taper off less quickly than theory predicts in the wings of the peak. This could be due to relatively unimportant omissions in our theory such as the finite wave-vector dependence of the intervalence-band susceptibility term. The other common feature of the spectra which is not predicted by the theory is the pronounced peak seen slightly below the unscreened LO-phonon energy. The origin of this peak is unclear. It is tempting to attribute it to a spatial averaging problem but for two reasons: Under such circumstances one might expect a peak at, or slightly above, the unscreened LO-phonon energy, not below it, and the fits obtained excepting this spurious peak are quite good and do not require any spatial averaging. The values of plasma density extracted from the fits for all delay times are given in the final column of Table I.

The plasma densities at the semiconductor surface as extracted from the Raman data are plotted as a function of the relative time delay between the peaks of the pump and probe pulses in Fig. 3. We modeled this behavior by solving a simple one-dimensional diffusion equation[20] for the spatial and temporal evolution of the plasma, using the measured parameters of our pump pulses as given above. The diffusion model assumed a constant, density-independent ambipolar diffusion coefficient of 5 cm^2/sec and a surface recombination velocity of 1.0×10^5 cm/sec. The ambipolar diffusion coefficient for InP based on electron and hole mobilities[20] of 4000 cm/V sec and 100 cm/V sec is 5 cm^2/sec, in good agreement with our results. Others[13] have measured surface recombination velocities as high as 2.4×10^4 cm/sec for doped n-type InP, so the value of 1.0×10^5 cm/sec does not seem unreasonable for a semi-insulating InP sample, as the trend is for the surface recombination velocity to decrease at higher doping levels.[21]

TABLE II. List of parameters used in calculations.

Symbol	Description	Value
m_e^*	Electron effective mass	$0.078m_0$
m_{LH}^*	Light-hole effective mass	$0.12m_0$
m_{HH}^*	Heavy-hole effective mass	$0.45m_0$
C	Faust-Henry coefficient	−0.46
Γ_l	Ionic damping constant	3 cm^{-1}
T	Temperature	300 K
ε_0	Static dielectric constant	12.35
ε_∞	High-frequency dielectric constant	9.53
ω_t	TO-phonon energy	303.5 cm^{-1}
ω_l	LO-phonon energy	345.5 cm^{-1}

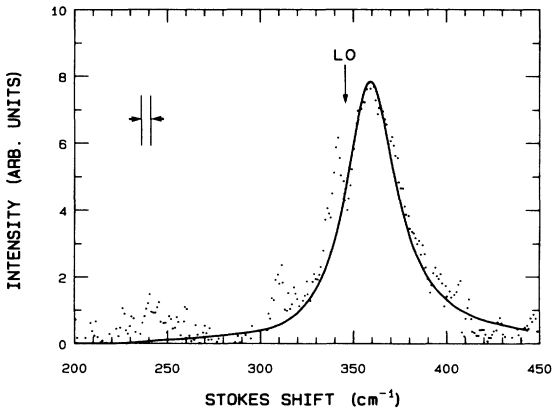

FIG. 2. The measured (dots) and calculated (solid line) coupled-mode spectrum for a pump-probe delay of 62 psec. The arrow indicates the energy of the unscreened LO phonon.

In conclusion, we have obtained the Raman spectra from coupled nonequilibrium electron-hole plasmon–LO-phonon modes in semi-insulating InP for plasma densities ranging from 0.1 to 5.0×10^{17} cm^{-3}. By using separate pump and probe beams, data free of temporal and spatial averaging were obtained for the first time. The spectra were fit using extensions to equilibrium coupled mode scattering theories to take account of the simultaneous presence of free electrons and free holes in a degenerate ($K=0$) valence band. The diffusion coefficient and surface recombination velocity of the plasma, as estimated by fitting the surface density versus time data with a simple diffusion model, are consistent with accepted values.

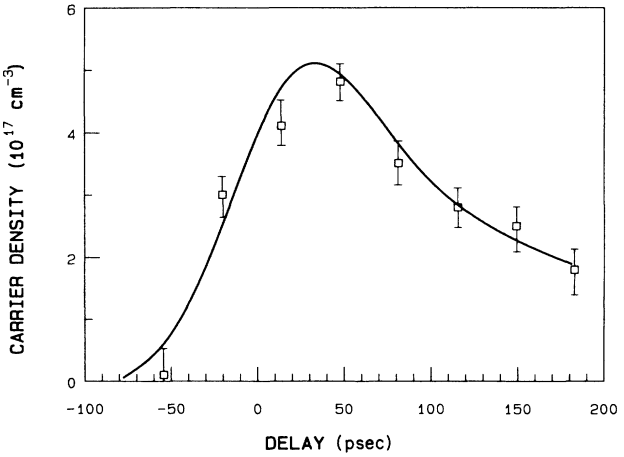

FIG. 3. The surface plasma density, as deduced from calculated fits of the Raman spectra, vs the relative delay of pump and probe pulses (□). The solid curve is the calculated temporal dependence of the surface plasma density (see text).

We wish to extend thanks to R. Normandin, P. Kelly, and P. Corkum from the National Research Council for many helpful discussions. Thanks also to M. Gallant of Bell Northern Research for providing the polished sample.

[1]D. von der Linde and R. Lambrich, Phys. Rev. Lett. **42**, 1090 (1979).

[2]C. L. Collins and P. Y. Yu, Phys. Rev. B **30**, 4501 (1984).

[3]J. C. Tsang, J. A. Kash, and S. S. Jha, Physica B **134**, 184 (1985); J. A. Kash, J. C. Tsang, and J. M. Hvam, Phys. Rev. Lett. **54**, 2151.

[4]R. Luzzi and A. R. Vasconcellos, J. Raman Spectrosc. **10**, 28 (1981); A. R. Vasconcellos and R. Luzzi, *ibid.* **14**, 39 (1983).

[5]P. M. Platzman and P. A. Wolff, *Solid State Physics* (Academic, New York, 1973), Suppl. 13.

[6]M. V. Klein, in *Light Scattering in Solids I,* edited by M. Cardona (Springer, New York, 1983).

[7]For a recent review of Raman scattering from photoexcited plasmas, see G. Abstreiter, M. Cardona, and A. Pinczuk, in *Light Scattering in Solids IV,* edited by M. Cardona and G. Guntherodt (Springer, New York, 1984).

[8]C. L. Collins and P. Y. Yu, Solid State Commun. **51**, 123 (1984).

[9]R. S. Turtelli and A. R. B. de Castro, Phys. Status Solidi B **93**, 811 (1979).

[10]H. Nather and L. Quagliano, J. Lumin. **30**, 50 (1985).

[11]A. Pinczuk, J. Shah, and P. A. Wolff, Phys. Rev. Lett. **47**, 1487 (1981).

[12]J. E. Kardontchik and E. Cohen, Phys. Rev. Lett. **42**, 669 (1979).

[13]T. Nakamura and T. Katoda, J. Appl. Phys. **55**, 3064 (1984).

[14]The jitter was estimated by comparing the cross- and autocorrelation widths of two separate dye laser beams pumped by the same YAG beam.

[15]D. T. Hon and W. L. Faust, Appl. Phys. **1**, 241 (1973).

[16]M. Klein, B. N. Ganguly, and P. J. Colwell, Phys. Rev. B **6**, 2380 (1972).

[17]M. Combescot and P. Nozières, Solid State Commun. **10**, 301 (1972).

[18]W. Bardyszewski, Solid State Commun. **57**, 873 (1986).

[19]See Klein, Ref. 6, pp. 156–158.

[20]J. F. Young and H. M. van Driel, Phys. Rev. B **26**, 2147 (1982).

[21]D. E. Aspnes, Surf. Sci. **132**, 406 (1983).